Subcycle Terahertz Nonlinear Optics

Xin Chai,[1] Xavier Ropagnol,[1,2] S. Mohsen Raeis-Zadeh,[3] Matthew Reid,[4]
Safieddin Safavi-Naeini,[3] and Tsuneyuki Ozaki[1,*]
[1]*INRS-EMT, Varennes, Québec, Canada J3X 1S2*
[2]*École technologie supérieur (ÉTS), Montreal, Québec, Canada H3C 1K3*
[3]*University of Waterloo, Waterloo, Ontario, Canada N2L 3G1*
[4]*University of Northern British Columbia, Prince George, British Columbia, Canada V2N 4Z9*

(Received 16 April 2018; published 1 October 2018)

The nonlinear interaction of subcycle electromagnetic radiation with matter is the current frontier in ultrafast nonlinear optics and high-field physics. Here, we investigate nonlinear optical effects induced by intense, subcycle terahertz radiation in a doped semiconductor. We observe a truncation of the half-cycle terahertz pulse and an emission of high-frequency terahertz photons. We attribute our observations to the abrupt current drop caused by strong intervalley scattering effects. By adding an extra half-cycle terahertz pulse with opposite polarity, we monitor the evolution of the nonlinear carrier dynamics during a quasi-single-cycle pulse. Our results demonstrate the differences between nonlinear effects for subcycle and multicycle terahertz pulses. It also suggests a new approach to subcycle control of terahertz waveforms, and the generation of high-order terahertz harmonics could be realized by using multicycle pulses.

DOI: 10.1103/PhysRevLett.121.143901

Advances in ultrafast optics continue to expand the frontiers of extreme nonlinear light-matter interactions into new regimes, both in time, intensity, and bandwidth [1–4]. The confinement of nonlinear interactions to a subcycle permits accurate tests of theories of various fundamental processes [5–9]. A half-cycle pulse is the ultimate of short pulses, allowing one to temporally confine the electromagnetic energy to generate high electric fields, and to control the nonlinear light-matter interaction by providing a unidirectional action on charged particles. Pulses with durations less than a single cycle possess a large coherent bandwidth, which could lead to experimental phenomena that are distinct compared with few-cycle pulses [5,10]. Nonlinear ultrafast experiments have been performed using single- and few-cycle pulses, in which subcycle nonlinearities are extracted using time-resolve techniques [5–9]. However, the subcycle regime of nonlinear optics remains difficult to reach, due to the lack of intense subcycle laser sources. In this Letter, we use an intense quasiunipolar terahertz pulse to study the nonlinear dynamics of an ensemble of carriers in the semiconductor and their impact on the reshaping of subcycle terahertz waveforms. We demonstrate that subcycle nonlinear optics differ from single-cycle and multicycle nonlinear optics, where in the latter cases the nonlinearities from different half cycles could interact considerably to modify the observed results.

The discrete spectrum observed in high-order harmonic generation (HHG) is the result of the interference between harmonic radiation generated at different half cycles. HHG has been observed using extremely intense multiterahertz pulses, which is explained by dynamical Bloch oscillations in bulk semiconductor material [7,8]. In the conventional terahertz window (between 0.1 and 3 THz), intraband Bloch oscillation becomes difficult to observe due to the lower peak field strengths and various scattering effects [3,7,11]. In particular, the intervalley scattering effect dominates the high-field responses of several semiconductors, which have been reported using different terahertz sources [12–18]. Intense terahertz transients accelerate the free carriers in the central valley of the conduction band and when the carriers acquire enough kinetic energy, they can be scattered into the side valleys, where the carriers possess heavier effective mass and higher scattering rates. Overall, it decreases the macroscopic terahertz conductivity and in turn leads to the observation of terahertz absorption bleaching [12–18]. However, such an effect should essentially take place within single half-cycle acceleration and a strongly distorted subcycle current density can then change the terahertz half-cycle waveform.

We performed nonlinear terahertz time-domain spectroscopy on an *n*-doped semiconductor $In_{0.57}Ga_{0.43}As$ thin film using a quasi-half-cycle terahertz pulse with a peak frequency less than 0.2 THz. The interdigitated large-aperture photoconductive antenna (ILAPCA) based terahertz source provides a half-cycle duration up to 580 fs [amplitude full width at the half maximum (FWHM)], which is much longer than the terahertz pulses used in similar studies [12–23]. With such long acceleration, we can tune the light-matter coupling from linear to nonlinear and turn on the terahertz waveform reshaping within the single half cycle.

Our interdigitated ZnSe LAPCA is composed of 35 identical electrodes (37 mm long and 0.3 mm wide) over

a total area of 12.25 cm^2. The LAPCA is photoexcited by an 8 mJ, 400 nm femtosecond pump pulse (~60 fs) at a repetition rate of 10 Hz. The electric field of the radiated terahertz pulse is controlled by varying the bias voltage on the antenna, which induces only very small distortions on the emitted terahertz pulse waveforms. The sample under study was positioned carefully at the terahertz focus for high-field transmission measurements at normal incidence and the transmitted electric field of the terahertz pulse is measured via electro-optic sampling in a 300 μm (110)-cut GaP crystal. Our $In_{0.53}Ga_{0.47}As$ sample consists of a 500-nm-thick n-type $In_{0.53}Ga_{0.47}As$ (100) epilayer with a doping concentration of approximately 2×10^{18} cm^{-3}. The $In_{0.53}Ga_{0.47}As$ thin film is grown by metal-oxide chemical vapor deposition on a lattice matched, 0.35-mm-thick semi-insulating InP substrate. The InP substrate has shown an overall terahertz transmission of 0.7 and nonlinear effects are not observed when the experiment is carried out on a bare substrate.

Figure 1(a) shows the transmitted terahertz waveforms through the bare substrate (E_{ref}) and semiconductor sample (E_{trans}) when the incident peak field is at 190 kV/cm. We observed high-frequency generation (HFG) with spectral amplitude enhancement from approximately 1 up to 2.5 THz. In the time domain [inset of Fig. 1(a)], a clear truncation of the half-cycle pulse is shown, where the front and rear part have been chopped after transmission through the sample.

To study the nonlinear effect, we varied the incident terahertz peak field E_{in} from 31 to 190 kV/cm. Figure 1(b) plots the transmitted terahertz peak fields and the half-cycle durations as a function of the incident field. The sample has shown linear responses at low fields and strong nonlinear transmission enhancement is observed at high fields. Meanwhile, the half-cycle duration maintains above 500 fs at low fields and decreases rapidly when the field is above 129 kV/cm, where transmissions greater than one have been observed at high frequencies [Fig. 1(c)]. The region of spectral amplitude enhancement enlarges with the field and covers the spectral range above 1 THz.

To understand the subcycle nonlinear carrier dynamics, we performed theoretical analysis in the time domain by using the thin-film transmission equation [13,19–23],

$$E_{\mathrm{trans}}(t) = \frac{1}{Y_0 + Y_S}[2Y_0 E_{\mathrm{in}}(t) - J(t)d]. \qquad (1)$$

Here, $d = 500$ nm is the thickness of the sample. $Y_0 = (377\,\Omega)^{-1}$ is the free-space admittance, and $Y_s = NY_0$ is the admittance of the substrate, in which N is the refractive index of InP [13]. The equation has been adjusted for

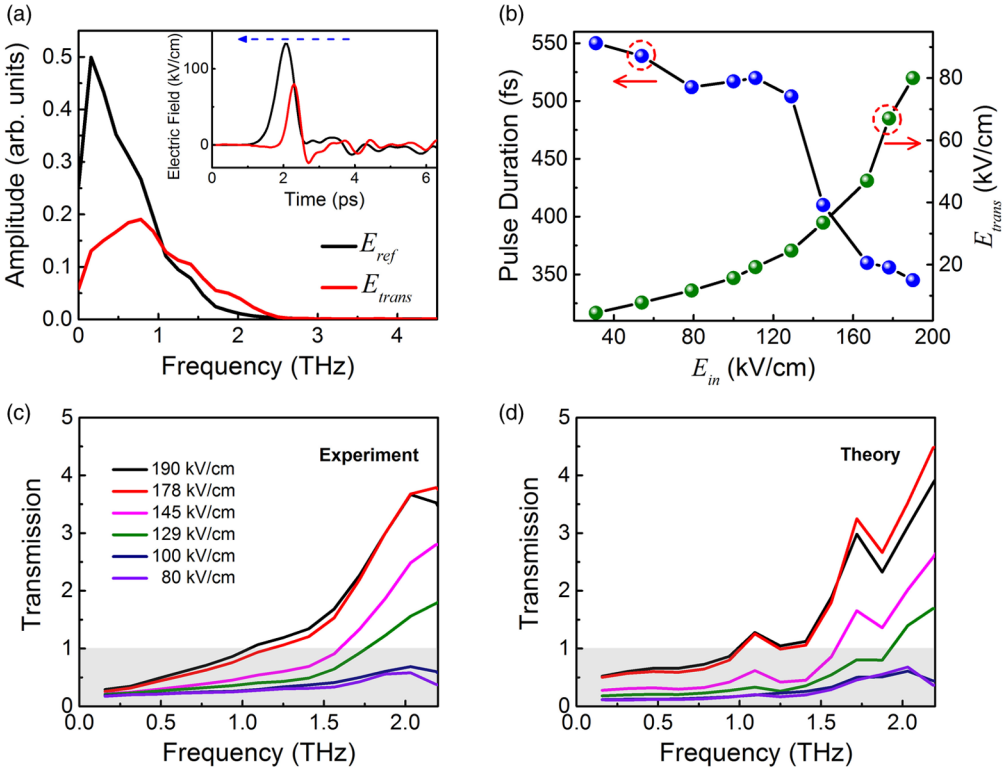

FIG. 1. (a) Amplitude spectra of the transmitted terahertz pulses through the bare substrate (E_{ref}) and the (In,Ga)As sample (E_{trans}) with the incident peak field of 190 kV/cm. Inset: corresponding terahertz waveforms, where the blue arrow indicates the propagation direction. (b) Measured field dependence of E_{trans} and half-cycle duration (amplitude FWHM) as a function of the incident peak field E_{in} measured in air. (c) Measured transmission spectra at various incident fields. The gray area corresponds to the transmission lower than 1. (d) Calculated transmission spectra based on the described model.

terahertz first incident to the substrate [24]. In the thin-film regime, all the carriers are assumed to experience the same driving field E_{trans}, which is 80 kV/cm when the incident peak field is at 190 kV/cm. As is apparent from this linear relation between the current density and the emitted field, an ultrafast nonlinear distortion on a periodic current density $J(t)$ should contain high-order harmonics of the driving frequency and a continuous high-frequency band could be generated when subcycle pulses are applied. To characterize the transient carrier dynamics, we used an analytical-band ensemble Monte Carlo approach as a solution of the Boltzmann transport equation [25–29]. The ballistic motion can be largely suppressed at high energies due to the relatively weak but slow-varying field in the picosecond range ($\omega_{0.15\ \mathrm{THz}}^{-1} \approx 1.07$ ps) [7,19]. The dynamics of each carrier in the ensemble were simulated simultaneously and $J(t)$ was determined by the average drift velocity.

Figure 1(d) shows the calculated terahertz transmissions for various field strengths. A continuous high-frequency band is generated due to the subcycle current drop, as shown in Fig. 2. This rapid drop in current density further causes a temporal shift of the transmitted terahertz peak. Here, all the terahertz pulses are measured from the same starting time. At high fields, the rear part of the half cycle experiences a much lower conductivity and in turn pushes the terahertz peak backwards in time. These observations are reproduced nicely by our time-domain analysis, in which a rapid crossover from drift energy to thermal energy dominant carrier motions takes place within the half-cycle pulse [25].

For coherent intraband carrier transport, an intense laser field can drive carriers to the edge of the Brillouin zone before scattering takes place, leading to Bloch oscillations in bulk material [7,31]. Charge carriers perform several oscillations during every half cycle of the laser and emit high-order harmonics [7,31]. Here, the current drop due to scattering causes a truncation of the half-cycle pulse and in turn increases the bandwidth of the transmitted pulse. However, the scattered hot carriers in the upper valleys possess much longer relaxation time [12,13,32]. Hence, the next half cycle should possess a nontrivial dependence on the field strength of the first half cycle, giving rise to distinct responses for single- and multicycle pulses. To experimentally demonstrate the different nonlinearities, we build a quasi-single-cycle terahertz pulse by using a binary phase mask on the same ILAPCA terahertz source [25,30].

We optimized the incident field strength of negative polarity (E_{neg}) to be equal to 80% that of positive polarity (E_{pos}). Transmitted peak fields [Fig. 3(e)] as well as the half-cycle duration [Fig. 3(f)] are extracted for both E_{pos} and E_{neg}. At low fields [region 1 in Fig. 3(f)], linear responses are obtained and the transmitted terahertz waveforms remain similar to the incident pulses with E_{neg} smaller than E_{pos}. When the peak field is increased to 105 kV/cm, we observe a clear amplitude increase for the negative field extreme [Fig. 3(b)], where E_{neg} becomes higher than E_{pos} after transmission. This observation can be seen more clearly by comparing the instantaneous intensities in the time domain, where the difference reaches a

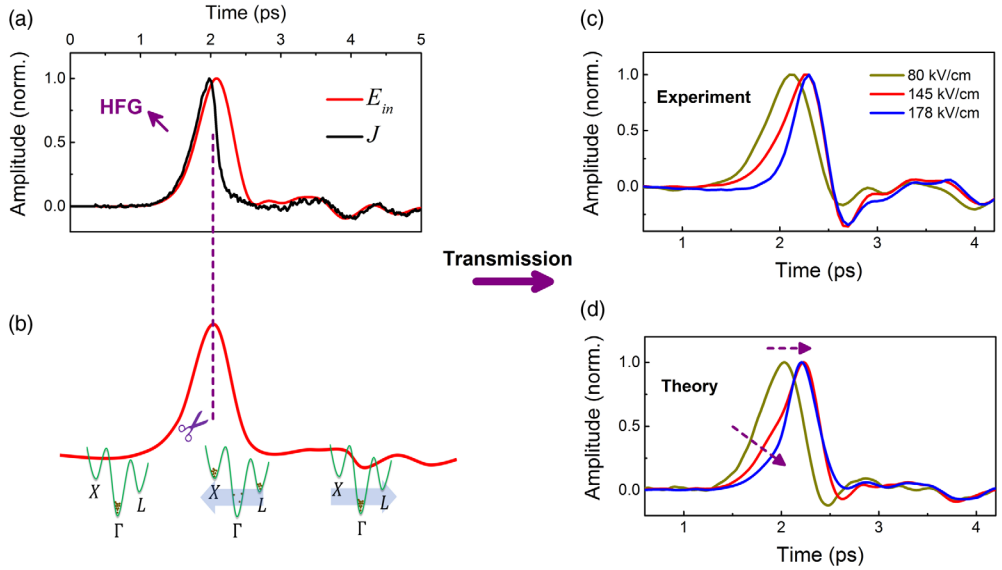

FIG. 2. (a) Incident terahertz waveform and the calculated current density with the field strength of 190 kV/cm. (b) Schematic of the experiment in momentum space: intense terahertz transient induces carrier intervalley scattering. The increased field strength leads to a damping of the subcycle current density and an increase in the total relaxation time. (c) Impact of current drop on the transmitted terahertz waveforms of three tested field strengths shown in Fig. 1. The transmitted waveforms are normalized by the corresponding peak values. (d) Normalized transmitted terahertz waves obtained from calculation.

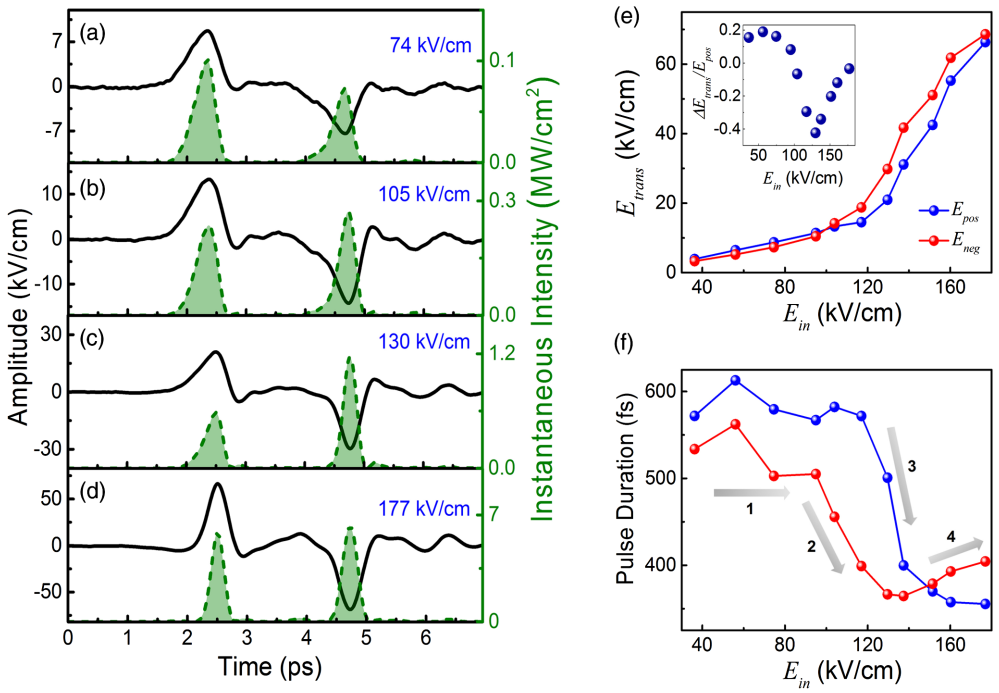

FIG. 3. Transmitted terahertz pulses (solid black curve) and the instantaneous terahertz intensity (broken green curve) at various incident fields of (a) 74 kV/cm, (b) 105 kV/cm, (c) 130 kV/cm, and (d) 177 kV/cm. (e) The transmitted fields of negative (E_{neg}) and positive extremes (E_{pos}) versus the incident field. Inset: $\Delta E_{\mathrm{trans}}/E_{\mathrm{pos}}$, where $\Delta E_{\mathrm{trans}} = E_{\mathrm{pos}} - E_{\mathrm{neg}}$. (f) field dependence of half-cycle durations (amplitude FWHM). Four field regions can be identified, representing: 1, the linear regime; 2, current truncation on the negative polarity; 3, current truncation on the positive polarity; and 4, pulse broadening of the negative polarity.

maximum when the incident field is at 130 kV/cm [Fig. 3(c)]. Meanwhile, the half-cycle duration of E_{neg} decreases from around 500 to 360 fs, while that of E_{pos} is still above 500 fs [region 2 in Fig. 3(f)]. This intriguing "reversal" of the transmitted pulse shape is caused by the residual carriers in the upper valleys after excitation by E_{pos}, which results in a higher E_{neg} that can rapidly decelerate and reaccelerate the remaining carriers in the Γ valley, subsequently rescattering them to the upper valleys. However, when E_{pos} is sufficiently intense [region 3 in Fig. 3(f)], $\Delta E_{\mathrm{trans}}/E_{\mathrm{pos}}$ starts to reduce and the pulse duration of E_{pos} decreases from 575 to less than 400 fs. This is consistent with the results using half-cycle pulses, where the current truncation leads to a shortening of the transmitted terahertz pulse. More interestingly, the half-cycle duration of E_{neg} starts to increase once the terahertz field is higher than 137 kV/cm, while that of the positive polarity continues to decrease [region 4 in Fig. 3(f)]. This is a direct result of the intervalley carrier dynamics induced by single-cycle pulses as verified by our calculation [25]. Weak current density during E_{neg} allows more low-frequency components to be transmitted through the sample and in turn increases the half-cycle duration.

In principle, intervalley scattering randomizes the momentum of different charge carriers and destroys the coherent transport. However, the total current density is determined by the collective motion of an ensemble of carriers. Within one half-cycle pulse, the total current density has shown an acceleration followed by an abrupt reduction [Fig. 2(a)]. From the excitation by the first half cycle, a distorted current that synchronizes with the driving terahertz fields can be generated, which could lead to discrete HHG when multicycle pulses are applied (see Supplemental Material [25]). Here, although the coherency of individual scattered particles is diminished by isotropic intervalley scattering, the overall nonlinear current density has shown coherent characteristics that vary in phase with the driven terahertz pulse. Macroscopically, this is similar to the terahertz coherent HHG in graphene, where a suppression in the temporal peaks of the current density is caused by the linear band dispersion, giving rise to the generation of odd harmonics in the transmitted terahertz wave [33,34].

For field-driven intraband Bloch oscillation, the number of oscillations within each half-cycle increases with the driving laser field [7,31]. However, the field dependence is considerably reduced for subcycle nonlinearities induced by nonparabolicity of the band dispersion [33,34] or by the current truncation due to carrier heating. The extent of nonparabolicity and the speed of carrier heating determines the efficiency and the optimum spectral range of HFG. As can be seen from our results [Figs. 1(b) and 3(f)], the reduction in the subcycle duration saturates gradually at

high fields for the studied $In_{0.57}Ga_{0.43}As$ sample. Therefore, low frequency terahertz sources [35], which possess much longer half-cycle duration, are more favorable here for the observation of HFG beyond their incident frequency range. In reality, depending on the desired functionality, the field at which the subcycle duration saturates can be controlled by tuning the carrier concentration, the thickness of the sample, or by using other semiconductor material that have different band structure, as well as mobility and speed of carrier heating and relaxation.

In conclusion, nonlinear interactions between subcycle terahertz pulse and intraband charge carriers lead to unique experimental observations with the emission of a continuum high-frequency terahertz spectrum. The nonlinearities of material evolve half cycle by half cycle along the entire terahertz waveform. Our investigations have demonstrated a new approach to subcycle control of terahertz high-frequency generation based on intraband carrier scattering effects. Our findings are important for future terahertz electronics and optoelectronics. Incoherent effects such as intervalley scattering could considerably alter the waveform of a subterahertz pulse, resulting in the generation of high-frequency components.

We would like to acknowledge the Natural Sciences and Engineering Research Council of Canada (NSERC), the Ministère de l'Enseignement supérieur, de la Recherche, de la Science et de la Technologie of Québec. We thank Axis-Photonique for their technical assistance with the pulsed high voltage source. We thank F. Vidal and J. Claustre for their help on the Monte Carlo simulation. We thank A. Laramée for the technical support on the 10 Hz beam line. We thank D. Cooke and M. Dignam for insightful discussions and appreciate M. Fareed for useful comments on the manuscript.

*To whom all correspondence should be addressed.
ozaki@emt.inrs.ca

[1] T. Brabec and F. Krausz, Rev. Mod. Phys. **72**, 545 (2000).
[2] F. Krausz and M. Ivanov, Rev. Mod. Phys. **81**, 163 (2009).
[3] T. Kampfrath, K. Tanaka, and K. A. Nelson, Nat. Photonics **7**, 680 (2013).
[4] P. B. Corkum and F. Krausz, Nat. Phys. **3**, 381 (2007).
[5] E. Goulielmakis, M. Schultze, M. Hofstetter, V. S. Yakovlev, J. Gagnon, M. Uiberacker, A. L. Aquila, E. M. Gullikson, D. T. Attwood, R. Kienberger, F. Krausz, and U. Kleineberg, Science **320**, 1614 (2008).
[6] G. Günter, A. A. Anappara, J. Hees, A. Sell, G. Biasiol, L. Sorba, S. De Liberato, C. Ciuti, A. Tredicucci, A. Leitenstorfer, and R. Huber, Nature (London) **458**, 178 (2009).
[7] O. Schubert, M. Hohenleutner, F. Langer, B. Urbanek, C. Lange, U. Huttner, D. Golde, T. Meier, M. Kira, S. W. Koch, and R. Huber, Nat. Photonics **8**, 119 (2014).
[8] M. Hohenleutner, F. Langer, O. Schubert, M. Knorr, U. Huttner, S. W. Koch, M. Kira, and R. Huber, Nature (London) **523**, 572 (2015).
[9] C. Riek, P. Sulzer, M. Seeger, A. S. Moskalenko, G. Burkard, D. V. Seletskiy, and A. Leitenstorfer, Nature (London) **541**, 376 (2017).
[10] A. F. Kemper, B. Moritz, J. K. Freericks, and T. P. Devereaux, New J. Phys. **15**, 023003 (2013).
[11] R. Ulbricht, E. Hendry, J. Shan, T. F. Heinz, and M. Bonn, Rev. Mod. Phys. **83**, 543 (2011).
[12] F. H. Su, F. Blanchard, G. Sharma, L. Razzari, A. Ayesheshim, T. L. Cocker, L. V. Titova, T. Ozaki, J. C. Kieffer, R. Morandotti, M. Reid, and F. A. Hegmann, Opt. Express **17**, 9620 (2009).
[13] L. Razzari, F. H. Su, G. Sharma, F. Blanchard, A. Ayesheshim, H. C. Bandulet, R. Morandotti, J. C. Kieffer, T. Ozaki, M. Reid, and F. A. Hegmann, Phys. Rev. B **79**, 193204 (2009).
[14] M. C. Hoffmann and D. Turchinovich, Appl. Phys. Lett. **96**, 151110 (2010).
[15] J. Hebling, M. C. Hoffmann, H. Y. Hwang, K.-L. Yeh, and K. A. Nelson, Phys. Rev. B **81**, 035201 (2010).
[16] I.-C. Ho and X. C. Zhang, Appl. Phys. Lett. **98**, 241908 (2011).
[17] D. Turchinovich, J. M. Hvam, and M. C. Hoffmann, Phys. Rev. B **85**, 201304 (2012).
[18] K. Fan, H. Y. Hwang, M. Liu, A. C. Strikwerda, A. Sternbach, J. Zhang, X. Zhao, X. Zhang, K. A. Nelson, and R. D. Averitt, Phys. Rev. Lett. **110**, 217404 (2013).
[19] W. Kuehn, P. Gaal, K. Reimann, M. Woerner, T. Elsaesser, and R. Hey, Phys. Rev. Lett. **104**, 146602 (2010).
[20] W. Kuehn, P. Gaal, K. Reimann, M. Woerner, T. Elsaesser, and R. Hey, Phys. Rev. B **82**, 075204 (2010).
[21] F. Blanchard, D. Golde, F. H. Su, L. Razzari, G. Sharma, R. Morandotti, T. Ozaki, M. Reid, M. Kira, S. W. Koch, and F. A. Hegmann, Phys. Rev. Lett. **107**, 107401 (2011).
[22] P. Bowlan, W. Kuehn, K. Reimann, M. Woerner, T. Elsaesser, R. Hey, and C. Flytzanis, Phys. Rev. Lett. **107**, 256602 (2011).
[23] P. Bowlan, W. Kuehn, K. Reimann, M. Woerner, T. Elsaesser, R. Hey, and C. Flytzanis, Phys. Rev. B **85**, 165206 (2012).
[24] A. T. Tarekegne, K. Iwaszczuk, M. Zalkovskij, A. C. Strikwerda, and P. U. Jepsen, New J. Phys. **17**, 043002 (2015).
[25] See Supplemental Material at http://link.aps.org/supplemental/10.1103/PhysRevLett.121.143901 which includes Refs. [13,26–30], for a discussion of the single-cycle terahertz generation, detailed theoretical model, HHG for single-cycle and multicycle terahertz pulses, and the calculated carrier dynamics.
[26] A. P. Long, P. H. Beton, and M. J. Kelly, J. Appl. Phys. **62**, 1842 (1987).
[27] M. Lundstrom, *Fundamentals of Carrier Transport* (Cambridge University Press, Cambridge, 2009).
[28] C. Jacoboni and L. Reggiani, Rev. Mod. Phys. **55**, 645 (1983).
[29] M. Mohamed, A. Bharthuar, and U. Ravaioli, DOI: 10.4231/D38C9R505 (2015).
[30] X. Ropagnol, R. Morandotti, T. Ozaki, and M. Reid, Opt. Lett. **36**, 2662 (2011).

[31] S. Ghimire, A. D. DiChiara, E. Sistrunk, P. Agostini, L. F. DiMauro, and D. A. Reis, Nat. Phys. **7**, 138 (2011).
[32] M. C. Hoffmann, J. Hebling, H. Y. Hwang, K.-L. Yeh, and K. A. Nelson, Phys. Rev. B **79**, 161201 (2009).
[33] I. Al-Naib, J. E. Sipe, and M. M. Dignam, Phys. Rev. B **90**, 245423 (2014).
[34] I. Al-Naib, M. Poschmann, and M. M. Dignam, Phys. Rev. B **91**, 205407 (2015).
[35] D. Zhang, A. Fallahi, M. Hemmer, X. Wu, M. Fakhari, Y. Hua, H. Cankaya, A.-L. Calendron, L. E. Zapata, N. H. Matlis, and F. X. Kärtner, Nat. Photonics **12**, 336 (2018).